JOURNAL OF GUIDANCE, CONTROL, AND DYNAMICS
Vol. 19, No. 6, November–December 1996

Optimality and Guidance for Planar Multiple-Burn Orbit Transfers

C.-H. Chuang,* Troy D. Goodson,† and Laura A. Ledsinger‡
Georgia Institute of Technology, Atlanta, Georgia 30332
and
John Hanson§
NASA Marshall Space Flight Center, Huntsville, Alabama 35812

An analysis of the second variation for extremal orbital transfers is presented, as well as a discussion of a multiple-burn guidance scheme that may be implemented for such transfers. The second variation analysis includes the examination of the conditions for free final time transfers. A continuous burn transfer is shown to have neighboring extremals through these conditions. An implicit guidance scheme is explored, which implements a neighboring optimal feedback guidance strategy to calculate thrust direction and thrust off-times. A new time-to-go formulation is introduced, which has improved performance for this transfer. This continuous burn guidance scheme is adapted to multiple-burn transfers. A two-burn guidance problem is simulated.

Nomenclature

$\boldsymbol{A}, \boldsymbol{B}, \boldsymbol{C}$	= coefficient matrices for a linear time-varying system, nondimensional (n.d.)
a	= semimajor axis, n.d.
d(−)	= total derivative of (−)
e	= eccentricity
$\boldsymbol{e}_T$	= thrust direction, n.d.
f	= system dynamics, $[\dot{r}, \dot{v}, \dot{m}]^T$
g_o	= gravitational acceleration at sea level, n.d.
H	= Hamiltonian function
H_s	= switching function
I_{sp}	= specific impulse of the motor, n.d.
J	= cost functional
L	= performance index
m	= mass, n.d.
$\boldsymbol{m}, \boldsymbol{n}, \alpha$	= sweepback vectors/variable for free final time, n.d.
$\boldsymbol{P}, \boldsymbol{S}, \boldsymbol{V}$	= sweepback matrices (fixed final time), n.d.
$\bar{\boldsymbol{P}}, \bar{\boldsymbol{S}}, \bar{\boldsymbol{V}}$	= sweepback matrices (free final time), n.d.
$\boldsymbol{r}$	= radius vector, $[x \ y]^T$, n.d.
T	= thrust magnitude, n.d.
t	= time, n.d.
$\boldsymbol{v}$	= velocity vector, $[u \ v]^T$, n.d.
Δ	= length of discretized interval
$\delta(-)$	= perturbation of (−)
θ or u	= control angle, n.d.
$\boldsymbol{\lambda}$	= Lagrange-multiplier time history, n.d.
μ	= gravitational constant, n.d.
$\nu_{1,2,3}$	= Lagrange multipliers for terminal constraints, n.d.
Φ	= scalar function of constraints
ϕ	= equality constraint
ψ	= constraining function
Ω	= transversality condition
$(-)_f$	= (−) at final time
$(-)_x$	= quantity at the switching time
$(-)_{x,y,u,v,m,\theta}$	= quantity associated with that certain state, control, state vector
$(-)_o$	= (−) at initial time
$\dot{(-)}$	= time derivative of (−)
$\bar{(-)}$	= nominal value of (−)

Received Oct. 30, 1995; revision received May 29, 1996; accepted for publication June 7, 1996.

*Assistant Professor, School of Aerospace Engineering. Senior Member AIAA.
†Ph.D. Candidate, School of Aerospace Engineering; currently Engineer, Jet Propulsion Laboratory, California Institute of Technology, Pasadena, CA 91109. Member AIAA.
‡Graduate Research Assistant, School of Aerospace Engineering.
§Aerospace Engineer, Flight Mechanics Branch. Member AIAA.

I. Introduction

THE conditions that result from analyzing the first variation of a cost functional are widely used. These are commonly referred to as the Euler–Lagrange equations, natural boundary conditions, and the transversality condition, when dealing with a free final time problem. Many problems require additional considerations; for example, the problem considered here, fuel-optimal orbit transfer, requires consideration of Pontryagin's maximum principle.

Many researchers have used the first variation to compute extremal solutions to the fuel-optimal orbit transfer problem. Some have used them to apply two-point boundary value problem solvers to optimization problems, forming indirect methods.[1–3] Others have used a partial set of the conditions to form hybrid indirect/direct methods where certain highly sensitive parameters are optimized directly.[4,5] To the knowledge of the authors, few have made use of the conditions related to the second variation of the cost functional of the fuel-optimal transfer problem, and none have been found to apply the second variation conditions to the multiple-burn problem. These provide sufficient conditions that, when met, declare an extremal solution as a locally weak optimal solution.

Once the second variation of the cost functional is verified so that it is known whether the sufficient conditions are met, the information obtained can then be used to implement a guidance scheme. Guidance is defined to be the determination of a way to follow a trajectory when presented with obstacles such as environmental disturbances or uncertainties in navigation data. Two different types of guidance schemes exist: implicit and explicit. Implicit guidance systems are characterized by the fact that the vehicle's motion must be precomputed on the ground and then compared with the actual motion. The equations that need to be solved are based upon the difference between these measured and precomputed values. The solutions to these equations are used in the vehicle's steering and velocity control. Explicit guidance systems are generalized by the fact that the vehicle's equations of motion are modeled and solved for by onboard computers during its motion. The solutions for the equations are solved continuously and are used to determine the difference between where the vehicle's current motion would eventually take the vehicle and its desired final destination. Commands are then generated to alleviate the anticipated error.

Existing guidance schemes have been presented in various papers. A guidance scheme that is implemented using a linear tangent law is presented by Sinha et al.[6] In a paper by Lu,[7] a general nonlinear

guidance law is developed using two different strategies. One strategy uses optimal control theory to generate a new optimal trajectory onboard from the start, whereas the other uses flight-path-restoring-guidance to bring the trajectory back to the nominal. A guidance scheme that is developed using inverse methods for unthrusted, lift-modulated vehicles along an optimal space curve is presented by Hough.[8] Linearized guidance laws applicable to many different types of space missions are presented by Tempelman.[9] These guidance laws are based on fixed and free final time arrivals. Naidu[10] presents a guidance scheme applicable to aeroassisted orbital transfers. This scheme is developed by implementing neighboring optimal guidance and linear quadratic regulator theory. Some interesting techniques for making the neighboring optimal guidance converge about the nominal path are introduced in a paper by Powers.[11]

The guidance scheme proposed in this paper is an implicit one that implements neighboring optimal feedback guidance. An implicit guidance system was chosen beause that type of guidance system handles disturbances well.[10] The neighboring optimal feedback guidance was chosen because it inherently uses the nominal solutions. Also, it has the advantage of being a feedback system, as opposed to open-loop guidance.

In this scheme, the initial orbit exit point is assumed to be perturbed from the nominal point, but the boundary condition, specifying the final orbit, is assumed to be unchanged. The goal is to use the controller to bring the trajectory back to the nominal path at some point and still deliver the spacecraft to the proper final orbit using minimal fuel.

This paper also introduces a new time-to-go scheme based on discretizing the optimal feedback gains. Although based on the same concepts of previous methods, this time-to-go scheme requires no iteration to calculate time-to-go as did previous methods.[12–14]

II. First Variation Considerations

The solution examined in this paper satisfies the conditions related to the first variation. In the next section, the conditions sufficient for declaring a minimizing solution will be checked for this transfer. The transfer examined in this paper is a two-burn transfer. To simplify initial analysis, a "new" nominal solution has been constructed from the original transfer. This new nominal solution is just a single-burn transfer; in fact, it is the last burn of the original trajectory.

Referring to Fig. 1, the singleburn that will be used for the initial analysis of this multiple-burn transfer is the thrust arc, which is located between the coast arc and the final orbit. This one-burn extremal solution has a fixed initial point and fixed transfer time, but the final point is constrained only in that it must lie on the final orbit. Specific details about Fig. 1 are elaborated upon in Sec. II.B.

A. First Variation Conditions

The first-order conditions for this problem have been stated many times[15] and will be given here only briefly. The optimization problem consists of a cost functional [Eq. (1)], state dynamics [Eqs. (2–4)], fixed initial point conditions [Eq. (5)], boundary conditions on the terminal point [Eq. (6)], and a Hamiltonian [Eq. (7)]; each of these is expressed as follows:

$$J = -m(t_f) \tag{1}$$

$$\dot{\boldsymbol{r}} = \boldsymbol{v} \tag{2}$$

$$\dot{\boldsymbol{v}} = (T/m)\boldsymbol{e}_T - (\mu/r^3)\boldsymbol{r} \tag{3}$$

$$\dot{m} = -\frac{T}{g_o I_{\text{sp}}} \tag{4}$$

$$\boldsymbol{r}(t_o) = \boldsymbol{r}_o, \qquad \boldsymbol{v}(t_o) = \boldsymbol{v}_o, \qquad m(t_o) = m_o \tag{5}$$

$$\begin{bmatrix}\psi_1\\ \psi_2\\ \psi_3\end{bmatrix} = \begin{bmatrix} xv - yu \\ (v^2 - \mu/r)x - (\boldsymbol{r}^T\boldsymbol{v})u \\ (v^2 - \mu/r)y - (\boldsymbol{r}^T\boldsymbol{v})v \end{bmatrix} - \begin{bmatrix} h \\ \mu e_x \\ \mu e_y \end{bmatrix} \tag{6}$$

$$H = \boldsymbol{\lambda}_r^T\boldsymbol{v} + \boldsymbol{\lambda}_v^T\left\{\frac{T}{m}\boldsymbol{e}_T - \frac{\mu}{r^3}\boldsymbol{r}\right\} - \lambda_m\frac{T}{g_o I_{\text{sp}}} \tag{7}$$

In Eq. (6), v is the velocity magnitude.

The term T is limited between zero and some maximum value $T_{\max}$. The Euler–Lagrange conditions are then

$$\boldsymbol{e}_T = -\boldsymbol{\lambda}_v/|\boldsymbol{\lambda}_v| \tag{8}$$

$$\dot{\boldsymbol{\lambda}}_r = \mu\left[\frac{\boldsymbol{\lambda}_v}{r^3} - 3\frac{(\boldsymbol{\lambda}_v^T\boldsymbol{r})\boldsymbol{r}}{r^5}\right] \tag{9}$$

$$\dot{\boldsymbol{\lambda}}_v = -\boldsymbol{\lambda}_r \tag{10}$$

$$\dot{\lambda}_m = (T/m^2)\boldsymbol{\lambda}_v^T\boldsymbol{e}T = (-T/m^2)|\boldsymbol{\lambda}_v| \tag{11}$$

where $\boldsymbol{\lambda}_r = [\lambda_x \ \lambda_y]^T$ and $\boldsymbol{\lambda}_v = [\lambda_u \ \lambda_v]^T$. The natural boundary conditions are

$$\lambda_x(t_f) = -\nu_2 w + \nu_3 v + \nu_4(v^2 + w^2 - \mu/r + \mu x^2/r^3) + \nu_5(\mu xy/r^3 - uv)|_{t=t_f} \tag{12}$$

$$\lambda_y(t_f) = \nu_1 w - \nu_3 u + \nu_4(\mu xy/r^3 - uv) + \nu_5(u^2 + w^2 - \mu/r + \mu y^2/r^3)|_{t=t_f} \tag{13}$$

$$\lambda_u(t_f) = \nu_2 z - \nu_3 y + \nu_4(-yv - zw) + \nu_5(2yu - xv)|_{t=t_f} \tag{14}$$

$$\lambda_v(t_f) = -\nu_1 z + \nu_3 x + \nu_4(2xv - uy) + \nu_5(-xu - zw)|_{t=t_f} \tag{15}$$

$$\lambda_m(t_f) = -1 \tag{16}$$

The conditions resulting from applying Pontryagin's minimum principle are

$$\begin{aligned} H_s &< 0, \qquad T = T_{\max} \\ H_s &> 0, \qquad T = 0 \end{aligned} \tag{17}$$

where

$$H_s = -\left(\frac{|\boldsymbol{\lambda}_v|}{m} + \frac{\lambda_m}{g_o I_{\text{sp}}}\right) \tag{18}$$

Note that when the time derivatives of H_s are zero, singular arc solutions may exist. The fact that such a singular arc does not exist for this problem has been checked numerically.[16]

The free final time problem will be considered here. For these extremal solutions, the final, or transfer, time is selected such that the transversality condition is satisfied; i.e., the Hamiltonian is zero at $t = t_f$,

$$H(t_f) = \boldsymbol{\lambda}_r^T\dot{\boldsymbol{r}} + \boldsymbol{\lambda}_v^T\dot{\boldsymbol{v}}|_{t=t_f} = 0 \tag{19}$$

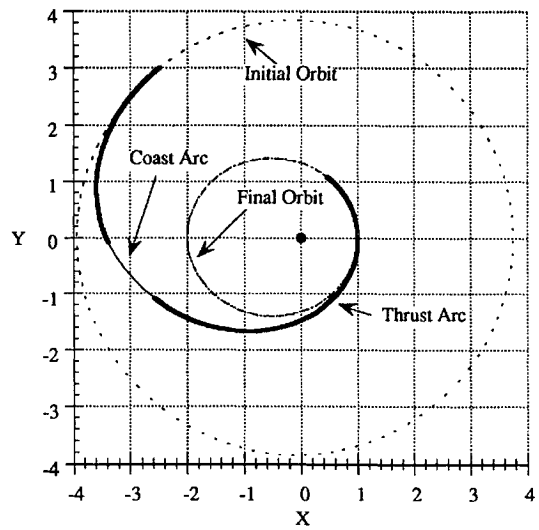

Fig. 1 Two-burn extremal orbit transfer solution with free final time.

In a previous paper[15] this problem was given as a maximization problem (maximization of the final mass). To conform to the convention used for the second variation,[16] it is now stated as a minimization problem. If an extremal solution to the maximization problem is given as state time history $\boldsymbol{x}(t)$, Lagrange-multiplier time history $\lambda(t)$, and Lagrange multipliers $\boldsymbol{\nu}$, associated with boundary conditions, then the extremal solution of the preceding minimization problem is $\boldsymbol{x}(t)$, $(-1) * \boldsymbol{\lambda}(t)$, and $(-1) * \boldsymbol{\nu}$.

Additionally, it makes more sense in the guidance problem to consider the control as the angle θ, rather than individual components of a unit vector. This simplifies the analysis because the control is now a scalar. Equation (8) may now be restated as

$$\tan(\theta) = -(\lambda_v/\lambda_u) \tag{20}$$

B. Extremal Solutions

All quantities associated with the solution presented here have been nondimensionalized so that $\mu = 1$ and will be presented here in that form. The transfer given in Fig. 1 has both the initial orbit exit point and final orbit entry points free. However, for the guidance problem it makes more physical sense to consider the initial orbit exit point as fixed and equal to the optimal choice, for it cannot be updated once the transfer has begun.

Any burn of any multiburn transfer may also be taken as a complete free final time transfer unto itself; this is a result of conditions elaborated upon in a previous work.[15] In this case, a one-burn transfer, identified as the thrust arc to the final orbit in Fig. 1, i.e., the last burn, will be used for initial analysis. The initial point can be chosen as the one at the very first instant (or shortly thereafter) of thrusting for the last burn. The final orbit exit point must remain unchanged. Obviously, for these choices the natural boundary conditions for the final orbit entry point are still satisfied. This one-burn transfer can then be considered as a new extremal solution, though to an orbit transfer problem with a different initial orbit.

Figure 1 displays a two-burn transfer, in fact a descending transfer, from an orbit with elements $a = 3.847$ and $e = 0.02378$ to a final orbit with elements $a = 1.5$ and $e = 0.3333$. The apses of the terminal orbits are aligned and lie on the x axis. The initial mass is 1.608 and the final mass is 1.1547 for a nominal transfer of 19.05 s long. The initial and final arguments of perigee are both 0 deg. The maximum thrust for the transfer is 0.03 with the value of $g_o I_{sp}$ being 1.313. This transfer has the transversality condition converged; therefore, it is a candidate fuel-optimal free final time solution.

III. Checking the Second Variation

Extensive derivation of the conditions for the second variation of the cost functional has already been detailed by Bryson and Ho.[16] Equations given in this section only summarize this work and extend it to the orbital transfer problem.

Considering the second variation of the augmented cost functional J, a new optimal control problem can be stated. In this new problem, the state is δx, the control δu, and the Lagrange multipliers are $\delta\lambda$ and $\mathrm{d}\nu$. The problem can be solved using a sweepback method. For the problem considered here, $x = [\boldsymbol{r}^T \ \boldsymbol{v}^T \ m]^T$ and $u = \theta$.

When the final time is unspecified, the transversality condition must be satisfied by the nominal solution. This condition is expressed as

$$\Omega(\boldsymbol{x}, \boldsymbol{u}, \boldsymbol{\nu}, t)|_{t=t_f} \equiv \left(\frac{\mathrm{d}\Phi}{\mathrm{d}t} + \boldsymbol{L}\right)_{t=t_f} = 0 \tag{21a}$$

where

$$\Phi = \phi(\boldsymbol{x}, t) + \boldsymbol{\nu}^T \psi(\boldsymbol{x}, t) \tag{21b}$$

$$\frac{\mathrm{d}\Phi}{\mathrm{d}t} = \frac{\partial\Phi}{\partial t} + \frac{\partial\Phi}{\partial \boldsymbol{x}}\dot{\boldsymbol{x}} \tag{21c}$$

In general, neighboring optimal feedback guidance allows the designer to consider changes in boundary conditions. No such changes are considered, assuming that the destination orbit was accurately planned well in advance. Formulation will be made later for both the fixed and free final time case.

The change in state and costate can be estimated with a linear time-varying dynamic system:

$$\delta\dot{\boldsymbol{x}} = \boldsymbol{A}(t)\delta\boldsymbol{x} - \boldsymbol{B}(t)\delta\boldsymbol{\lambda} \tag{22}$$

$$\delta\dot{\boldsymbol{\lambda}} = -\boldsymbol{C}(t)\delta\boldsymbol{x} - \boldsymbol{A}^T(t)\delta\boldsymbol{\lambda} \tag{23}$$

where

$$\boldsymbol{A}(t) = \boldsymbol{f}_x - \boldsymbol{f}_u H_{uu}^{-1} \boldsymbol{H}_{ux} \tag{24}$$

$$\boldsymbol{B}(t) = \boldsymbol{f}_u H_{uu}^{-1} \boldsymbol{f}_u^T \tag{25}$$

$$\boldsymbol{C}(t) = \boldsymbol{H}_{xx} - \boldsymbol{H}_{xu} H_{uu}^{-1} \boldsymbol{H}_{ux} \tag{26}$$

Evaluating the terms in Eqs. (22–26), for orbital transfer, the partial differential equations for the dynamics and for the Hamiltonian are

$$\boldsymbol{f}_x = \begin{bmatrix} 0 & 0 & -(\mu/r^3) - (3\mu x^2/r^5) & (3\mu xy/r^5) & 0 \\ 0 & 0 & (3\mu xy/r^5) & -(\mu/r^3) - (3\mu y^2/r^5) & 0 \\ 1 & 0 & 0 & 0 & 0 \\ 0 & 1 & 0 & 0 & 0 \\ 0 & 0 & -(T/m)\cos(\theta) & -(T/m)\sin(\theta) & 0 \end{bmatrix}^T \tag{27}$$

$$\boldsymbol{f}_\theta = \begin{bmatrix} 0 \\ 0 \\ -(T/m)\sin(\theta) \\ (T/m)\cos(\theta) \\ 0 \end{bmatrix} \tag{28}$$

$$\boldsymbol{H}_{xx} = \begin{Bmatrix} -\mu\left[\dfrac{-3(3\lambda_u x + \lambda_v y)}{r^5} + \dfrac{15(\lambda_v^T \boldsymbol{r})x^2}{r^7}\right] & -\mu\left[\dfrac{-3(\lambda_u y + \lambda_v x)}{r^5} + \dfrac{15(\lambda_v^T \boldsymbol{r})xy}{r^7}\right] & 0 & 0 & 0 \\ -\mu\left[\dfrac{-3(\lambda_u y + \lambda_v x)}{r^5} + \dfrac{15(\lambda_v^T \boldsymbol{r})xy}{r^7}\right] & -\mu\left[\dfrac{-3(3\lambda_v y + \lambda_u x)}{r^5} + \dfrac{15(\lambda_v^T \boldsymbol{r})y^2}{r^7}\right] & 0 & 0 & 0 \\ 0 & 0 & 0 & 0 & 0 \\ 0 & 0 & 0 & 0 & 0 \\ 0 & 0 & 0 & 0 & 2(T/m^3)|\boldsymbol{\lambda}_v| \end{Bmatrix} \tag{29}$$

$$H_{\theta\theta} = (T/m)|\boldsymbol{\lambda}_v| \tag{30}$$

$$H_{\theta X} = 0 \tag{31}$$

Using the sweepback method for nonlinear terminal constraints, as is the case for this development, the form for $\delta\lambda$ and $\delta\psi$ can be written as

$$\delta\lambda(t) = \bar{P}(t)\delta x(t) + \bar{S}(t)\,d\nu \tag{32}$$

$$\delta\psi = \bar{S}^T(t)\delta x(t) + \bar{V}(t)\,d\nu \tag{33}$$

Since $\delta\psi = 0$, as dictated by the boundary conditions, $d\nu$ can be written as

$$d\nu = -\bar{V}^{-1}(t_o)\bar{S}^t(t_o)\delta x(t_o) \tag{34}$$

$$f = -\nu_3 v(t_f) \tag{41d}$$

$$g = \nu_1 - \nu_2 u(t_f) + 2\nu_3 v(t_f) \tag{41e}$$

$$i = -\nu_1 - \nu_2 v(t_f) + 2\nu_3 u(t_f) \tag{41f}$$

$$j = -\nu_2 u(t_f) \tag{41g}$$

$$k = 2\nu_3 y(t_f) \tag{41h}$$

$$l = -\nu_3 x(t_f) - \nu_2 y(t_f) \tag{41i}$$

$$q = 2\nu_2 x(t_f) \tag{41j}$$

$$S(t_f) = \begin{bmatrix} v(t_f) & v^2(t_f) - \dfrac{\mu}{r} + \dfrac{\mu x^2(t_f)}{r^3} & \dfrac{x(t_f)y(t_f)}{r^3} - u(t_f)v(t_f) \\ -u(t_f) & \dfrac{x(t_f)y(t_f)}{r^3} - u(t_f)v(t_f) & u^2(t_f) - \dfrac{\mu}{r} + \dfrac{\mu y^2(t_f)}{r^3} \\ -y(t_f) & -y(t_f)v(t_f) & 2y(t_f)u(t_f) - x(t_f)v(t_f) \\ x(t_f) & 2x(t_f)v(t_f) - u(t_f)y(t_f) & -x(t_f)u(t_f) \\ 0 & 0 & 0 \end{bmatrix} \tag{42}$$

The matrices $\bar{P}$, $\bar{S}$, and $\bar{V}$ are computed using the following relations:

$$\bar{P} = P - (mm^T/\alpha) \tag{35}$$

$$\bar{S} = S - (mn^T/\alpha) \tag{36}$$

$$\bar{V} = V - (nn^T/\alpha) \tag{37}$$

Now the matrices P, S, V, m, n, and α are computed from a dynamic system. The boundary condition equations are given by

$$P(t_f) = \left[\phi_{xx} + \left(\nu^T\psi_x\right)_x\right]_{t=t_f} \tag{38}$$

$$S(t_f) = \left[\psi_x^T\right]_{t=t_f} \tag{39}$$

$$V(t_f) = 0 \tag{40}$$

where in the development for the orbital transfer these are

$$P(t_f) = \begin{bmatrix} b & c & f & g & 0 \\ c & d & i & j & 0 \\ f & i & k & l & 0 \\ g & j & l & q & 0 \\ 0 & 0 & 0 & 0 & 0 \end{bmatrix} \tag{41}$$

$$b = \nu_2\mu\left[\frac{x(t_f)}{r^3} - \frac{3x^3(t_f)}{r^5} + \frac{2x(t_f)}{r^3}\right] + \nu_3\mu\left[\frac{y(t_f)}{r^3} - \frac{3x^2(t_f)y(t_f)}{r^5}\right] \tag{41a}$$

$$c = \nu_2\mu\left[\frac{y(t_f)}{r^3} - \frac{3x^2(t_f)y(t_f)}{r^5}\right] + \nu_3\mu\left[\frac{x(t_f)}{r^3} - \frac{3x(t_f)y^2(t_f)}{r^5}\right] \tag{41b}$$

$$d = \nu_3\mu\left[\frac{y(t_f)}{r^3} - \frac{3y^3(t_f)}{r^5} + \frac{2y(t_f)}{r^3}\right] + \nu_2\mu\left[\frac{x(t_f)}{r^3} - \frac{3x(t_f)y^2(t_f)}{r^5}\right] \tag{41c}$$

Following from the assumptions expressed as Eqs. (32) and (33), the following nonlinear equations for P, S, and V must be integrated backwards. The results will be used to check the sufficient conditions governing a minimizing solution,

$$\dot{P} = -PA - A^TP + PBP - C \tag{43}$$

$$\dot{S} = -(A^T - PB)S \tag{44}$$

$$\dot{V} = S^TBS \tag{45}$$

$$\dot{m} = -(A^T - PB)m, \qquad m(t_f) = \left(\frac{d\Omega}{dx}\right)^T_{t=t_f} \tag{46}$$

$$\dot{n} = S^TBm, \qquad n(t_f) = \left(\frac{d\psi}{dt}\right)_{t=t_f} \tag{47}$$

$$\dot{\alpha} = m^TBm, \qquad \alpha(t_f) = \left(\frac{d\Omega}{dt}\right)_{t=t_f} \tag{48}$$

The sufficient conditions for a minimizing solution can now be stated as follows.

Convexity condition:

$$H_{\theta\theta}(t) > 0 \qquad \text{for} \qquad t_o \le t \le t_f \tag{49}$$

Normality condition:

$$\bar{V}^{-1}(t) \qquad \text{exists for} \qquad t_o \le t < t_f \tag{50a}$$

$$\alpha^{-1}(t) \qquad \text{exists for} \qquad t_o \le t < t_f \tag{50b}$$

Conjugate point condition:

$$\bar{P}(t) - \bar{S}(t)\bar{V}^{-1}(t)\bar{S}^T(t) \qquad \text{finite for} \qquad t_o \le t < t_f \tag{51}$$

The convexity condition is satisfied for any transfer satisfying the choice of control. This can be seen by noting that Eq. (30) is positive definite, irrespective of the time history for the Lagrange multipliers.

The term $\bar{V}$ was found to be negative definite in the required interval. Also, $\alpha(t)$ was found to be positive definite in the required interval. Since the normality condition requires that the inverse of $\bar{V}$ and $\alpha(t)$ exists in the interval, this solution is normal. The elements of the conjugate point matrix were found to be bounded in the required interval, and then they grew asymptotically at the final time. Therefore, this solution satisfies the sufficient conditions for minimizing the cost functional with free transfer time.

IV. Neighboring Optimal Feedback Guidance

Conveniently, construction of a neighboring optimal feedback guidance law uses the same information as that required to check the second variation of the cost functional. As a result, much of the derivation required of the guidance law has been stated already. The remaining discussion will describe how to form the feedback control law and adjust the equations of the bang-bang control for multiple-burn transfers in a feedback law.

The control $\delta\theta$ for the free final time problem can be found using

$$\delta\theta(t) = -H_{\theta\theta}^{-1}\left[\left(f_u^T\bar{P}\right)\delta x + f_u^T\bar{S}\,\mathrm{d}\nu\right]$$
$$= -H_{\theta\theta}^{-1}\left[f_u^T\left(\bar{P} - \bar{S}\bar{V}^{-1}\bar{S}^T\right)\right]\delta x \qquad (52)$$

and the change in the final time $\mathrm{d}t_f$ is

$$\mathrm{d}t_f = -\{[(\boldsymbol{m}^T/\alpha) - (\boldsymbol{n}^T/\alpha)\bar{V}^{-1}\bar{S}^T]\}\delta x \qquad (53)$$

Evaluating $\mathrm{d}t_f$ determines when the thrust will be turned off to complete the transfer.

Note that this continuous feedback law has been constructed by estimating $\mathrm{d}\nu$ at each instant of time. The feedback law depends on $\boldsymbol{P}$, $\boldsymbol{S}$, and $\boldsymbol{V}$ as functions of time. A particular advantage of the sweepback method is the solution of $P(t_o)$, $S(t_o)$, and $V(t_o)$, allowing the guidance law to store these values and propagate them forward to the current time to calculate the current feedback gain. The feedback gain may be propagated by integration or more practically by interpolation between stored values. Use of this control should keep the trajectory on a neighboring optimal solution and deliver the spacecraft to the required orbit in the specified transfer time.

The block diagram for the feedback controller needed for neighboring optimal feedback guidance is shown in Fig. 2, where $\Lambda_1(t)$ is the feedback gain for the $\delta(\theta)$ equation.

A. Time-to-Go Implementation

Since this problem is a free final time problem, the possibility exists that the final time will increase and the preceding simulation will "run out of gains"; this is a familiar issue for neighboring optimal feedback guidance. The approach used in this study is based on discretizing the gains by N time nodes $\{t_1, \ldots, t_i, \ldots, t_N\}$, where t_N is earlier than the nominal t_f. The gains at the nominal t_f would be infinite and impractical to store. Both the gains for calculating d_{tf} [see Eq. (53)] and for $\delta\theta$ [see Eq. (52)] are then calculated at any time by linear interpolation between stored values.

Although the basic premises are the same, this time-to-go formulation differs in various ways from those summarized by Bauer et al.[14] Where previous methods iterate to find the indexed time needed on the neighboring path to equate time-to-go's on the neighboring and nominal paths, the method presented here calculates that indexed time with no iteration necessary [Eqs. (54) and (55)]. Also, previous methods have used an approximation of $\mathrm{d}t_f$, whereas this method uses the entire quantity found in Eq. (53).

To consider time-to-go, the guidance must make active use of the $\mathrm{d}t_f$ estimation. Since both the nominal and the actual trajectories start at t_1, $\mathrm{d}t_{f1}$ can be initially calculated with the gains at that time. The length of the first guidance interval is then found by relating it to the estimated time-to-go:

$$\Delta t_{s1} = \frac{t_f + \mathrm{d}t_{f1}}{t_f}(t_2 - t_1) \qquad (54)$$

Then, at the end of the $i-1$th guidance interval, the gains at t_i are used to calculate $\mathrm{d}t_{fi}$. Using this information, the length of the ith guidance interval can be computed as

$$\Delta t_{si} = \frac{t_f + \mathrm{d}t_{fi} - \sum_{j=1}^{i-1}\Delta t_{sj}}{t_f - t_i}(t_{i+1} - t_i) \qquad (55)$$

This continues until Δt_{is} is computed as zero or a negative number or until $i = N$. When $i = N$, the Nth gain is used for the entire interval $\Delta t S_N$. Again note here that the reason the Nth gain is used for the entire last interval is because otherwise the gains would become infinite and storage of such gains would be difficult. In using such an approximation, a loss of optimality occurs; however, it is a small loss and will not greatly affect the end results. When the Nth interval ends, the guidance scheme is finished.

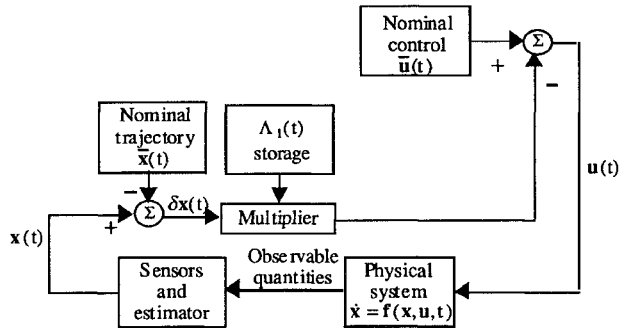

Fig. 2 Diagram of neighboring optimal feedback controller implementation.[15]

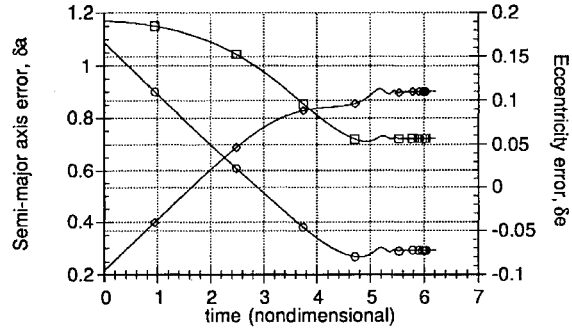

Fig. 3 Plot of boundary condition error for continuous guidance: ○, δa; □, δe-x component; and ◇, δe-y component.

The aforementioned scheme can be summarized with this list:

1) Use nominal t_i and calculate the comparative time on the neighboring path by use of Eq. (55).

2) Calculate $\mathrm{d}\theta$ and $\mathrm{d}t_f$ at t_i by using Eqs. (52) and (53) with interpolated values of the variables in these equations. These values are found by a linear interpolation between stored nominal values.

3) Continue the procedure until Eq. (55) equals to zero or becomes negative.

Figures 3 and 4 compare guidance performance with and without this time-to-go formulation. The curves represent the time history of the boundary condition error, i.e., Eq. (6) evaluated continuously. Figure 3 makes continuous use of the gains but indexes these gains at the current actual time without calculating $\mathrm{d}t_f$. For the perturbation simulated, the transfer time needs to increase, and this first scheme must terminate prematurely. Figure 4 makes use of the discretized gains and time-to-go formulation. This simulation also incorporates a practical saturation limit on the size of the gains. Upon comparison of these two plots, an improvement is evident as a result of the time-to-go formulation. The boundary condition error in Fig. 4 is less than that in Fig. 3, although still not exactly zero because of the small loss of optimality at the end of discretization as previously stated. Also, where there appears to be a chattering at the final time in Fig. 3, none is evidenced in Fig. 4. Therefore, this is both a practical and superior implementation of the continuous burn guidance.

B. Multiple-Burn Guidance

The guidance for multiple burns can also be discretized. For the two-burn case, discretized guidance using time-to-go is used for the first burn. The guidance algorithm will place the spacecraft on the intermediate transfer orbit via the neighboring optimal trajectory. Since the cost on this coast arc is zero, the spacecraft can coast on this arc until it reaches the point at which the next burn is to start. Once the spacecraft reaches this point, discretized guidance using time-to-go can be used again for the second burn. The boundary conditions for the second burn should than be satisfied by the neighboring path. Obviously, there would be a jump in the gain matrices between

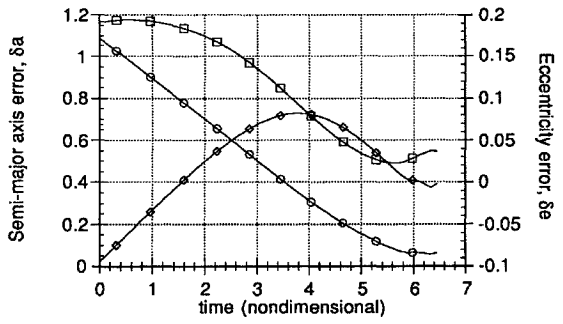

Fig. 4 Plot of boundary condition error for discrete guidance with time-to-go: ○, δa; □, δe-x component; and ◇, δe-y component.

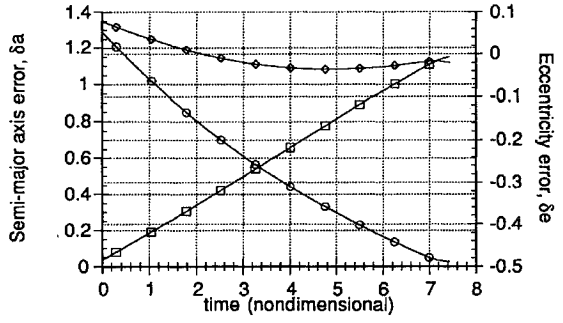

Fig. 5 Plot of boundary condition error for discrete guidance during the first burn: ○, δa; □, δe-x component; and ◇, δe-y component.

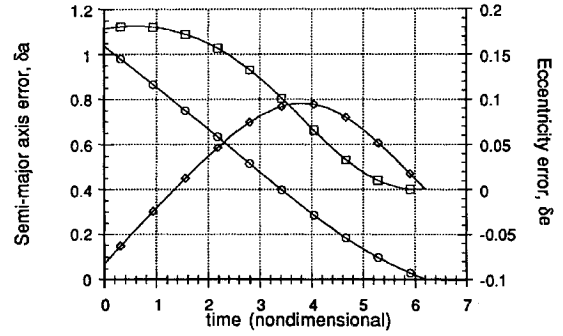

Fig. 6 Plot of boundary condition error for discrete guidance during the second burn (continuation of Fig. 5): ○, δa; □, δe-x component; and ◇, δe-y component.

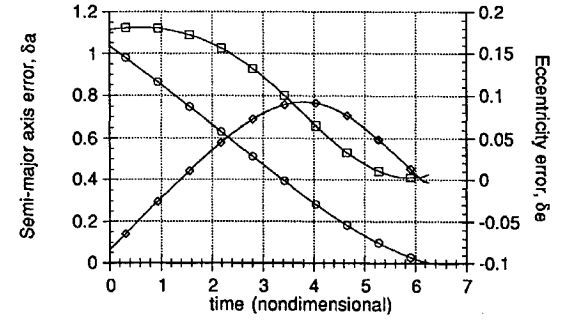

Fig. 7 Plot of boundary condition error for discrete guidance during the second burn for error in x: ○, δa; □, δe-x component; and ◇, δe-y component.

burns, but this is not a point of major concern since the multiple-burn transfer is handled as if it were numerous one-burn transfers. Thus, the gains are separate and not dependent from one burn to the next.

When there are many burns, this guidance scheme can be extended in a straightforward manner.

C. Multiple-Burn Guidance Simulation

The guidance scheme detailed earlier was used to recover the two-burn transfer of Fig. 1 in the presence of an initial perturbation.

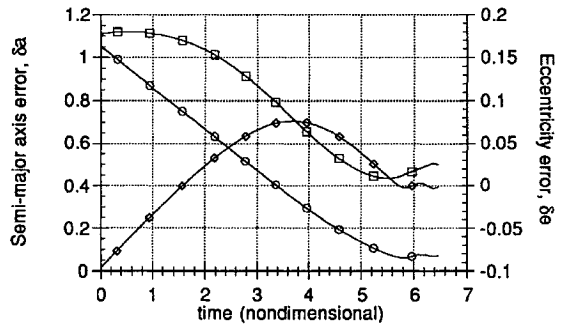

Fig. 8 Plot of boundary condition error for discrete guidance during the second burn for error in u: ○, δa; □, δe-x component; and ◇, δe-y component.

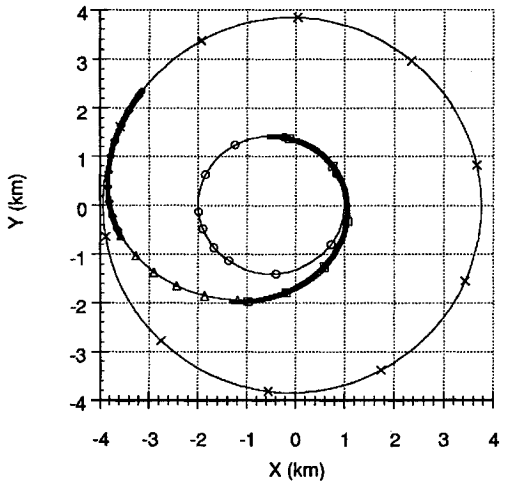

Fig. 9 Plot of the two-burn orbit transfer with initial perturbation: ○, final orbit; ♦, first burn; ×, initial orbit; □, second burn; and △, coast arc.

Figure 5 shows the boundary condition errors for the first burn given an initial perturbation of each of the states of 10^{-3} in nondimensionalized units. The boundary conditions are satisfied rather well for this burn. The resulting boundary condition errors for the second burn are quite small, as shown in Fig. 6.

Figures 7 and 8 show the boundary condition errors during the second burn for a perturbation of the same magnitude as earlier in only the x position and the u velocity, respectively. Note that the error in the boundary conditions is slightly greater in Fig. 8. This suggests that the spacecraft is more sensitive to disturbances in the u velocity than in the x position.

The resulting complete orbit transfer trajectory is shown in Fig. 9. This plot corresponds to the boundary condition errors as shown in Figs. 5 and 6.

V. Conclusions

Satisfaction of the sufficient conditions for an extremal orbit transfer trajectory has been shown. The neighboring optimal feedback guidance has been shown to reduce error in the trajectory. Furthermore, a guidance scheme utilizing time-to-go, and therefore appropriate to the free final time problem, has been shown to perform even better. This improved guidance scheme has been formulated for the multiple-burn problem. The preliminary simulation results show this practical scheme to be effective.

References

[1]Brusch, R. G., and Vincent, T. L., "Low-Thrust, Minimum-Fuel, Orbital Transfers," *Astronautica Acta*, Vol. 16, No. 1, pp. 65–74.

[2]Edelbaum, T. N., Sackett, L. L., and Malchow, H. L., "Optimal Low Thrust Geocentric Transfer," AIAA Paper 73-1074, Nov. 1973.

[3]Redding, D. C., and Breakwell, J., "Optimal Low-Thrust Transfers to Synchronous Orbit," *Journal of Guidance, Control, and Dynamics*, Vol. 7, No. 2, 1984, pp. 148–155.

[4]Zondervan, K. P., Wood, L. J., and Caughey, T. K., "Optimal Low-Thrust, Three-Burn Orbit Transfers with Large Plane Changes," *Journal of the Astronautical Sciences*, Vol. 32, No. 3, 1984, pp. 407–427.

[5]Anderson, G. M., and Smith, E. A., "A Combined Gradient/Neighboring Extremal Algorithm for the Calculation of Optimal Transfer Trajectories Between Noncoplanar Orbits Using a Constant Low Thrust Rocket," *Journal of the Astronautical Sciences*, Vol. 23, No. 3, 1984, pp. 225–239.

[6]Sinha, S. K., Shrivastava, S. K., Bhat, M. S., and Prabhu, K. S., "Optimal Explicit Guidance for Three-Dimensional Launch Trajectory," *Acta Astronautica*, Vol. 9, No. 2, 1989, pp. 115–125.

[7]Lu, P., "A General Nonlinear Guidance Law," AIAA Paper 94-3632, Aug. 1994.

[8]Hough, M. E., "Explicit Guidance Along an Optimal Space Curve," *Journal of Guidance, Control, and Dynamics*, Vol. 12, No. 4, 1989, pp. 495–504.

[9]Tempelman, W., "Linear Guidance Laws for Space Missions," *Journal of Guidance, Control, and Dynamics*, Vol. 9, No. 4, 1986, pp. 495–502.

[10]Naidu, D. S., *Aeroassisted Orbital Transfer: Guidance and Control Strategies*, Springer–Verlag, New York, 1994.

[11]Powers, W. F., "Techniques for Improved Convergence in Neighboring Optimal Guidance," *AIAA Journal*, Vol. 8, No. 12, 1970, pp. 2235–2241.

[12]Speyer, J. L., and Bryson, A. E., "A Neighboring Optimum Feedback Control Scheme Based on Estimated Time-to-Go with Application to Re-Entry Flight Paths," *AIAA Journal*, Vol. 6, No. 5, 1968, pp. 769–776.

[13]Wood, L. J., "Perturbation Guidance for Minimum Time Flight Paths of Spacecraft," AIAA Paper 72-915, Sept. 1972.

[14]Bauer, T. P., Wood, L. J., and Caughey, T. K., "Gain Indexing Schemes for Low-Thrust Perturbation Guidance," *Journal of Guidance, Control, and Dynamics*, Vol. 6, No. 6, 1983, pp. 518–525.

[15]Chuang, C.-H., Goodson, T. D., and Hanson, J., "Computation of Optimal Low- and Medium-Thrust Orbit Transfers," *Proceedings of the AIAA Guidance, Navigation, and Control Conference*, AIAA, Washington, DC, 1993, pp. 1391–1402.

[16]Bryson, A. E., and Ho, Y.-C., *Applied Optimal Control*, Taylor and Francis, Philadelphia, PA, 1975.